Hard-and-soft phosphinoxide receptors for f-element binding: structure and photophysical properties of europium(III) complexes†

Nataliya E. Borisova,*[a,b] Anastasia V. Kharcheva,[a,c] Svetlana V. Patsaeva,[c] Leonid A. Korotkov,[a] Sergey Bakaev,[a] Marina D. Reshetova,[a] Konstantin A. Lyssenko,[b] Elena V. Belova[d] and Boris F. Myasoedov[d]

New phosphinoyl-containing tetradentate heterocycles preorganised for metal ion binding were designed and prepared in high yields. The X-ray structures of two allied phosphinoyl-bearing 2,2′-bipyridyl and phenanthroline ligands, as well as closely related structures of 2,6-bis(diphenylphosphinoyl)pyridine and 9-(diphenylphosphinoyl)-1,10-phenanthroline-2-one, are reported. Complexes of nitrates of several lanthanides and trifluoroacetate of Eu(III) with two phosphinoyl-bearing 2,2′-bipyridyl and phenanthroline ligands were isolated and characterised. The first structures of lanthanide complexes with phosphinoyl-bearing 2,2′-bipyridyl and phenanthroline ligands are reported. The nature of the counter-ion is crucial for the coordination environment of the metal ion. The photophysical properties of the complexes differing in both the nature of the ligand and counter-ion were investigated. The photophysical properties of the complexes are strongly ligand- and counter-ion-dependent. Absorbance and luminescence excitation spectra of complexes showed main peaks in the UV range which correspond to the absorption of light by the ligand and these are ligand-dependent. Luminescence spectra of complexes show typical europium emission in the red region with a high quantum yield, which corresponds to the transitions $^5D_0 \rightarrow ^7F_J$ ($J = 0$–6). The value of deviation of the components of $^5D_0 \rightarrow ^7F_2$ and $^5D_0 \rightarrow ^7F_1$ transitions from the inversion centre shows a larger dependence on the counter-ion than on the nature of the ligand. The value of the luminescence quantum yield is larger for europium complexes with 2,2′-bipyridyl-based ligands and NO_3 counter-ions than for complexes with phenanthroline-based ligands and NO_3 counter-ions. A low dependence of the luminescence lifetime of Eu complexes on the nature of the ligand has been demonstrated: values in the solid state were in the range 1.1–2.0 ms.

[a]*Department of Chemistry, M.V. Lomonosov Moscow State University 1/3 Leninskie Gory, 119991 Moscow, Russian Federation. E-mail: borisova.nataliya@gmail.com; Fax: +7 495 939 0290*
[b]*N.A. Nesmeyanov Institute of Organoelement Compounds, 28 Vavilov Str., Moscow, Russian Federation. E-mail: kostya@xray.ineos.ac.ru*
[c]*Faculty of Physics, Lomonosov Moscow State University, 1/2 Leninskie Gory, 119991 Moscow, Russian Federation. E-mail: harcheva.anastasiya@physics.msu.ru*
[d]*A.N. Frumkin Institute of Physical Chemistry and Electrochemistry, RAS 31 Leninsky prospect, 119071 Moscow, Russian Federation. E-mail: mar@ipc.rssi.ru*
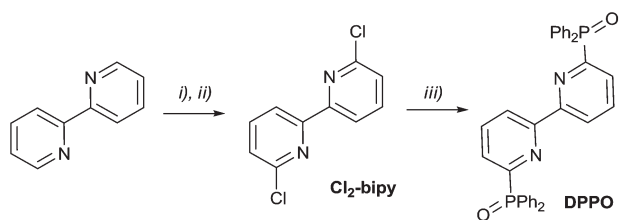
†Electronic supplementary information (ESI) available. CCDC 1521997–1522002. For ESI and crystallographic data in CIF or other electronic format see DOI: 10.1039/c6dt04681a

Introduction

Growing research efforts in the field of rare earth element (REE) complexes with bipyridine-type ligands are associated with their outstanding potential from the viewpoint of their fundamental and practical applications.[1–13] Extended variation

capabilities of supramolecular structures, as well as modification of peripheral positions of heterocycles, allow fine tuning of the molecular properties required for high technology applications. The high coordination numbers of lanthanide ions provide alternative methods for the modification of the properties of complexes by varying the counter-ion coordinated to the metal centre. This opens several new applications for already known complexes.[14,15] So the use of trifluoroacetate complexes provides a path for the preparation of several highly intense luminescent systems.[15–17] *N,O*-Polydentate hard-and-soft heterocyclic compounds attract attention as ligands for REE complexes due to their distinguished photophysical[5,18–20] and magnetic[21] properties and also due to their ability to discriminate ions of f-elements by their size.[22–33] Over several years we have designed novel types of *N,N′,O,O′*-tetradentate bypyridyl-based reagents for the selective separation of actinides from lanthanides[9,34–37] – a significant radiochemical problem in the field of closed nuclear fuel
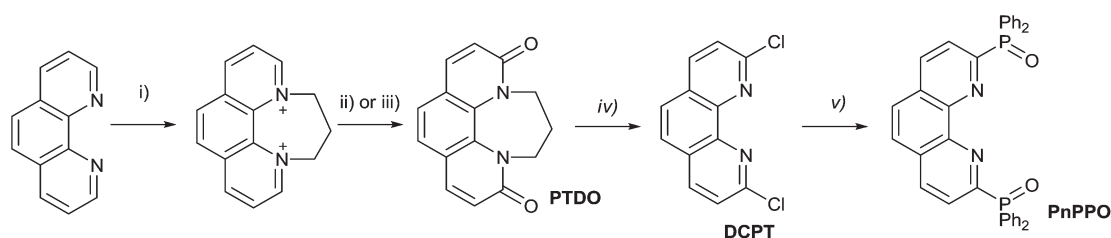
cycle development.[38] REE complexes with this new type of ligand possess promising photophysical properties which have been studied in detail along with the structure of the complexes.[39] In this work we combine hard-donor phosphinoxide groups with a soft heterocyclic framework. We investigate N,N',O,O'-tetradentate bypyridyl-based phosphinoxide compounds as ligands for lanthanide ions. The ligands bearing phosphinoxide groups together with a pyridine structural motif show intense solvent and counter-ion dependent luminescence.[40–42] In such complexes the energy transfer occurs from the ligand to the metal presumably via the pyridine (or other heterocycle) N–Ln coordination bond, but the emitted complexes have never been structurally characterised. There is one example of a structurally characterized coordination polymer of the REE complex, the pyridine-based phosphinoxide ligands, which have no metal ion coordination with the pyridine ring.[43,44] The coordination of lanthanide ions with a heterocyclic five-ring moiety simultaneously with the phosphinoxide-group exists in 4,5-bis(diphenyl)phosphoranyl-1,2,3-triazolate-based complexes with REEs.[45] Here we report studies on the complexation of the europium ion with two N,N',O,O'-tetradentate planar 2,2′-bypiridine-type systems both tuned by preorganisation of the ligand. Moreover, investigation of the correlation between the nature of the counter-ion and photophysical properties was performed by the introduction of a nitrate or trifluoroacetate counter-ion.

Results and discussion

The preparation of phosphinoxide-decorated 2,2′-bipyridyl starts from 6,6′-dibromo-2,2′-bipyridine which is available mostly by 2,6-dibromopyridine coupling.[46] We introduced dichloro-substituted heterocycles as alternative building blocks for the construction of phosphinoxide-containing ligands. Dichloro derivatives are usually readily available for a wide range of heterocycles such as 2,2′-bipyridine[47] and o-phenanthroline[48,49] and can be easily transformed into corresponding bis(diphenylphosphinoxides) by the reaction with Ph₂PNa (Schemes 1 and 2).

Oxidation of the commercially available 2,2′-bipyridyl with in situ generated peracetic acid leads to 2,2′-bipyridine-N,N'-dioxide. The latter was converted into **Cl₂-bipy** using PCl₅ in POCl₃.[47] The reaction of **Cl₂-bipy** with sodium diphenylphosphide under an inert atmosphere and subsequent oxidation of the mixture with hydrogen peroxide provided the target phosphinoxide **DPPO** in a preparative yield of 52%.
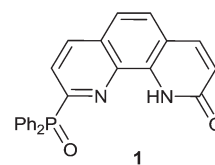
Synthesis of phenanthroline-2,9-bis(diphenylphosphinoxide) (**PnPPO**) is shown in Scheme 2. Contrary to the method initially proposed for quaternisation, which consisted of heating 1,3-dibromopropane and phenanthroline in nitrobenzene at 120 °C which led to the target salt in 70% yield,[49] we used bromobenzene as a solvent and 4 h heating at 115 °C gave a yellow precipitate of the target salt with quantitative yield. Furthermore, oxidation of the quaternary salt in air in the presence of alkoxides in the corresponding alcohol (EtOH/EtONa, tBuOH/tBuOK) gave **PTDO** in 81% and 75% yields, respectively. The product reacted with the POCl₃/PCl₅ mixture under reflux for 8 h to form **DCPT**.[49] After treatment with Ph₂PNa and subsequent oxidation with 5% H₂O₂, **DCPT** was converted to **PnPPO** in 70% yield. The reaction at 0 °C was complicated by the formation of a side product: the partial hydrolysis of phenanthroline chloride occurred (**1**). The diphenylphosphide ion assisted dealkylation of alkoxysubstituted pyridine was a major product of the reaction with the corresponding 2-chloropyridine.[50]

Analytical and spectroscopic characteristics are consistent with the suggested structure. The P═O fragment in both compounds is evidenced by IR spectroscopy (1202 and

Scheme 1 (i) H₂O₂, AcOH, reflux; (ii) POCl₃, PCl₅, reflux; then H₂O, 65%; (iii) Ph₂PNa, dioxane, 0 °C, RT overnight; then H₂O₂ (10%), 80%.

Scheme 2 (i) PhBr, 115 °C, 4 h, 100%; (ii) air, tBuOK/tBuOH, 75%; (iii) air, EtONa/EtOH 91%; (iv) POCl₃, PCl₅, reflux; then H₂O, 82%; (iii) Ph₂PNa, dioxane, −18 °C, RT overnight, then H₂O₂ (5%), 70%.

1200 cm^{-1}) and ^{31}P NMR. The phosphorus chemical shift (21.3 ppm in **DPPO** and 31.5 ppm in **PnPPO**) confirms the presence of the phosphine oxide group. Two doublets for the geminal carbons in the ^{13}C NMR spectrum (156.37–155.06 ppm with $^{1}J_{P-C(Py)}$ = 132.0 Hz and 132.71–131.67 ppm with $^{1}J_{P-C(Ph)}$ = 132.0 Hz) are in keeping with the structure of **DPPO**. The **DPPO** ^{1}H NMR spectrum agrees with the spectrum described earlier.[50] The ^{1}H NMR spectrum of **DPPO** is simplified by protonation. Addition of a drop of strong acid (H$_2$SO$_4$) leads to the separation of most of the signals: the d.d. signal at 8.32 ppm corresponds to 3′-protons of bipyridyl, d.t. at 7.96 ppm is related to the 4′-proton of bipyridyl and the last 5′-proton of hetero-aromatics is a part of the multiplet at 7.46 ppm. At the same time, protonation leads to a shift of the phosphorus ^{31}P NMR signal to 21.86 ppm. The ^{1}H NMR of **PnPPO** also supports the bis(phosphinoxide) structure, but the signals are more separated than those for **DPPO**. The protons of the common benzene ring are shifted to 7.70 ppm, and the protons at positions 3 and 8 and positions 4 and 7 form two doublets at 8.02 and 7.63 ppm, respectively. Structures are also supported by mass spectroscopy and elemental analysis.

The structures of the phosphinoxide-bearing ligands were studied by X-ray analysis (Fig. 1, Table 1). Structures of phos-phinoxide-bearing ligands, **DPPO** and **PnPPO**, are shown in Fig. 1. A striking feature of these ligands is the unfavourable conformation for metal ion binding: both diphenylphosphine-groups are unfolded relative to the pyridine ring in *anti*-conformation. The dihedral angles between the P=O group and the pyridine ring are close to 180° for both of the ligands (Table 1).

This feature can be considered as a general peculiarity of the 2-pyridinephosphineoxide-type ligands. We also tested the structure of 2,6-bis(diphenylphosphine)pyridine oxide (**PyPPO**) prepared according to a known procedure from commercially available 2,6-dibrimopyridine,[50] and the structure of 9-diphenyl-phosphinephenanthrolin-2-one oxide **1** (Fig. 2). Both show *anti*-conformation of the P=O group relative to the pyridine ring (Table 1). At this moment it is still unclear if this feature is typical for all pyridine-containing phenylphosphinoxides, or whether this conformation is limited only to diphenyl-phosphinoxide-bearing pyridines.

The length of P–O bonds is approximately 1.49 Å for all investigated ligands. This distance is considerably greater than that found in Me$_3$PO (1.44 Å),[51] but is in good agreement with the P–O bond length for uncoordinated diphenylphosphino-xide groups in 4,5-bis(diphenylphosphoranyl)-1,2,3-triazolate (1.465(5) to 1.485(5) Å (ref. 45) and 1.497(2) (ref. 52)). P–C$_{Py}$

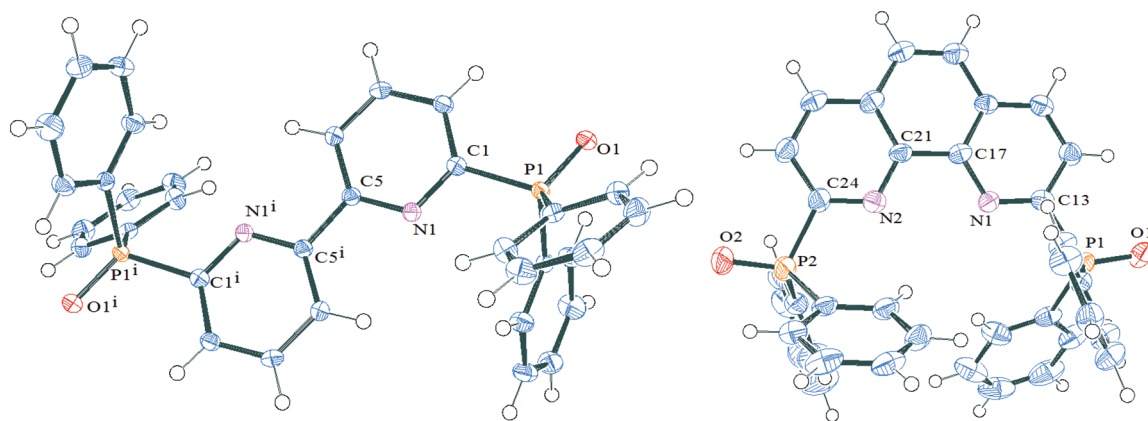**Fig. 1** ORTEPs of phosphinoxides **DPPO** and **PnPPO** with thermal ellipsoids at 50% level for all non-hydrogen atoms. Solvent molecules are omitted for clarity. Other figures are available in the ESI.†

Table 1 Selected geometry parameters (Å or °) for phosphinoxide ligands and their complexes

|	**PyPPO**	**DPPO**	**PnPPO**	**1**	**DPPOGd**	**PnPPOEu**
O=P–C$_{Py}$–N$_{Py}$ angle	−173.69(12)	169.28(14)	176.5(3)	−176.32(18)	−4.6(6)	−9.6(7)
	−171.02(12)		173.8(3)		28.1(6)	12.3(7)
N–C$_{Py}$–C$_{Py}$–N angle	—	180.0(2)	−4.4(6)	−3.3(4)	−22.4(9)	1(1)
P=O bond length	1.4877(13)	1.4877(15)	1.491(3)	1.4848(19)	1.503(5)	1.500(7)
	1.4923(12)		1.490(3)		1.507(5)	1.495(7)
P–C$_{Py}$ bond length	1.8190(17)	1.820(2)	1.827(4)	1.830(3)	1.827(7)	1.820(8)
	1.8243(17)		1.820(5)		1.809(7)	1.822(8)
O–P–C$_{Py}$ angle	111.42(8)	111.74(9)	110.9(2)	111.66(12)	106.9(9)	107.1(4)
	110.80(7)		110.5(2)		108.4(3)	107.3(4)
C$_{Py}$–C$_{Py}$ bond length	—	1.490(3)	1.450(6)	1.433(3)	1.479(10)	1.45(1)
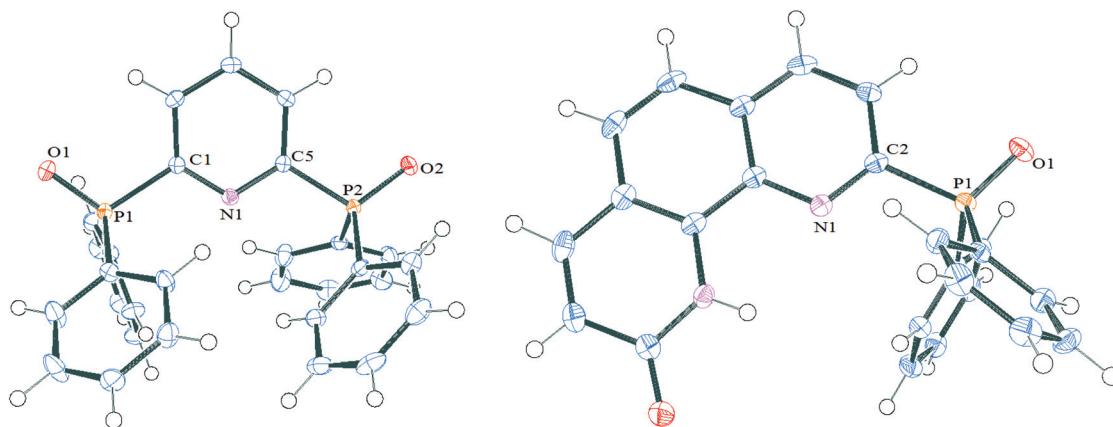
Fig. 2 ORTEPs of 2,6-bis(diphenylphosphinoxide)pyridine and 9-diphenylphosphinephenanthrolin-2-one oxide **1** with thermal ellipsoids at 50% level for all non-hydrogen atoms. Solvent molecules are omitted for clarity. Other figures are available in the ESI.†

bond lengths are about 1.82 Å, which is close to the corresponding length of the heterocycle-phosphinoxide C–P bond found earlier.[45,52] Both phosphorus atoms are near tetrahedral, and the corresponding angles are presented in Table 1 and ESI.†

The **DPPO** and **PnPPO** molecules do not form hydrogen bonded solvates in crystals. In contrast, **PyPPO** and phosphinoxide **1** show hydrogen bonding, either with water molecules, or during dimerization. Water molecules form strong hydrogen bonds with one of the phosphinoxide groups (2.14 Å H⋯O, O–H⋯O angle 172°, see the ESI†). Partly hydrolysed phosphinoxide **1** in the crystal form dimerises by strong hydrogen bonding (distance 2.937(3) Å, N–H⋯O angle 155(3), see in the ESI†) between the C=O oxygen atom and N–H hydrogen. Phosphinoxide **1** crystal packs by C–H⋯π stacking interactions (2.488 Å) between the phenyl rings of phosphinoxide moieties of neighbouring molecules.

In spite of the unfavourable arrangement of the donor atoms, both tetradentate phosphinoxide-bearing ligands readily form complexes with lanthanides (Scheme 3).

Diphenylphosphinoxides **DPPO** and **PnPPO** react rapidly with 4f-element salts in acetonitrile under reflux with the formation of corresponding mononuclear complexes of a general composition **LLnX₃**, where Ln is La, Eu, Gd or Er. MALDI-TOF mass spectrometry confirms the formation of mononuclear complexes; the mass spectra possess characteristic peaks of composition **LLnX₂⁺** for both ligands and all metal ion salts in accordance with earlier observations.[39] A striking feature of europium complexes with **DPPO** and **PnPPO** is the presence of peaks corresponding to an unusual composition **LLnX⁺**, which is attributed to hypothetical reduction of the europium species. All observed signals exhibit the expected characteristic isotopic distribution patterns. The fragmentation of trifluoroacetate complexes is more complicated. The decomposition of the fluorinated counter-ion leads to a fluorine anion, which is able to replace TFA⁻ in the complex and form mixed ions with compositions **LEuTFAF⁺** and **LEuF₂⁺**.
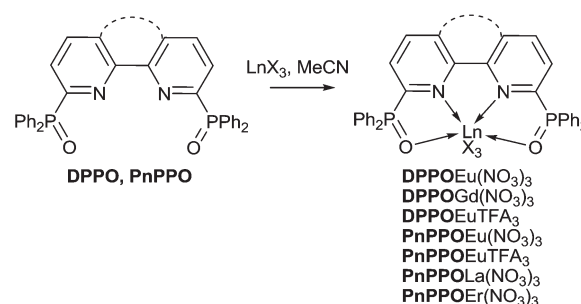
Scheme 3

The IR spectra provide more information about the structures of the complexes. The intense band near 1200 cm⁻¹, corresponding to the P=O stretching, is very sensitive to metal ion coordination.[18] We observed a significant lowering of the P=O band frequency from near 1200 to 1144 cm⁻¹ which confirmed the coordination of the metal ions to the phosphinoyl group. For the complexes with metal ion nitrates the N=O bands for NO₃ anions, which were observed near 1476 cm⁻¹ for all complexes, are extremely informative. Less intense bands corresponding to symmetrical and asymmetrical deformation O–N–O vibrations in the NO₃ anions were also observed.

The structure of the complexes of **DPPO** (**DPPOGd(NO₃)₃**, Fig. 3) and **PnPPO** (**PnPPOEu(TFA)₃·H₂O**, Fig. 4) with both nitrate and TFA counter-ions were studied by X-ray single-crystal diffraction (Tables 1 and 2). Both complexes are mononuclear and consist of one ligand coordinated to the metal ion in a tetradentate manner. Both complexes show coordination of the metal ion to the oxygen atoms of the phosphinoyl groups and to the nitrogen atoms of the pyridine heterocycle, supported by the formation of a five-membered metallocycle. The latter leads to elongation of the P=O bond (from 1.4877 in **DPPO** and 1.490 in **PnPPO** to 1.503 or 1.507 in **DPPOGd** and
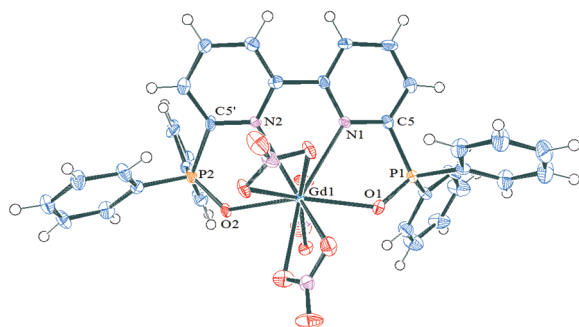
Fig. 3 ORTEPs of complex **DPPO**Gd(NO$_3$)$_3$ with thermal ellipsoids at 50% level for all non-hydrogen atoms. Hydrogen atoms and solvent molecules are omitted for clarity. Other figures are available in the ESI.†
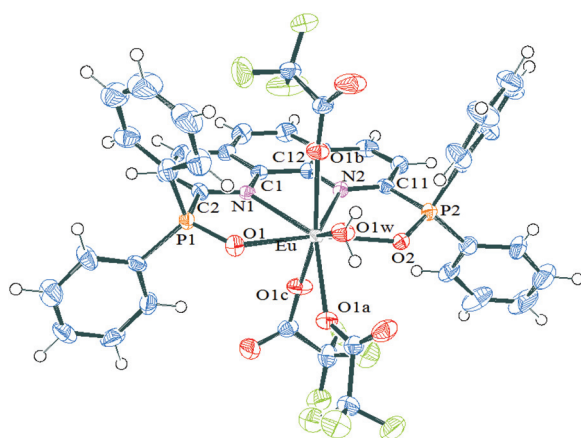

Fig. 4 ORTEPs of complex **PnPPO**Eu(TFA)$_3$·H$_2$O with thermal ellipsoids at 50% level for all non-hydrogen atoms. Solvent molecules are omitted for clarity. Other figures are available in the ESI.†

Table 2 Selected bond lengths (Å) in the coordination environment of metal ions for phosphinoxide complexes

	DPPOGd(NO$_3$)$_3$	**PnPPO**Eu(TFA)$_3$
Ln–N	2.665(5); 2.708(6)	2.662(7); 2.638(6)
Ln–O$_p$	2.359(5); 2.388(5)	2.331(6); 2.345(7)
Ln–O$_{anion}$	2.457(5); 2.477(5); 2.482(5);	2.389(4); 2.306(7);
	2.498(5); 2.501(5); 2.533(5)	2.319(5)
N–Ln–N	60.06(17)	61.4(2)
O$_p$–Ln–O$_p$	154.03(16)	162.6(2)
Eu–OH$_2$		2.431(6)

1.500 or 1.495 in **PnPPO**Eu, see Table 1). The P–O bond lengths are within the typical range.[45] A corresponding shift of IR bands was observed (*vide supra*). In contrast, the C–N bond in heterocycles does not undergo such changes (see the ESI†). The phosphorus atoms undergo tetrahedral distortion, which leads to a reduction in the O–P–C$_{Py}$ angles from about 111° to 107° (Table 1). The phosphinoyl groups are all are rotated

around the C$_{Py}$–P bond to adopt the conformation needed for metal ion binding. The O=P–C$_{Py}$–N$_{Py}$ torsion angles significantly diminish. The complexes are reorganised differently depending on the nature of the ligand. **DPPO** undergoes twisting in both the phosphinoyl group and the bipyridyl moiety. The angle between the two pyridine rings is 22.4(9)°, but the angles for the two Ph$_2$PO-groups are significantly different. One of the phosphinoyl groups lies near the plane of the heterocycle (−4.6(6)°) but the second is twisted from the plane to form a 28.1(6)° angle. In contrast, **PnPPO** undergoes relatively symmetrical distortion and the two phosphinoyl groups form a dihedral angle close to each other: −9.6(7) and 12.3(7)°.

The nature of the counter-ion has a crucial effect on the structure of the complexes: the nitrato complex possesses the decacoordinated gadolinium ion while the trifluoroacetato-complex shows an octacoordinated europium ion in a distorted bicapped-trigonalantiprismatic environment (Fig. 4). In **PnPPO**Eu(TFA)$_3$ the O(2), O(1B), O(1W) and O(1A), O(1C), O(1) atoms form two bases of the prisms while the nitrogen atoms serve as two caps. The bridging nature of the nitrato groups leads to a higher coordination number of the lanthanide ion; in contrast the monodentate coordination of the trifluoro-acetato-groups gives rise to additional coordination of a water molecule to the Eu ion.

The Ln–O,N distances are significantly shorter for the octa-coordinated lanthanide ion than for the decacoordinated lanthanide ion, both for the ligand and the counter-ion (Table 2). So the metal ion enters deeper into the cavity of the tetradentate ligand for **PnPPO**Eu(TFA)$_3$ than for **DPPO**Gd (NO$_3$)$_3$. The latter has an impact on the N–Ln–N and O$_p$–Ln–O$_p$ biting angles: the angles for the Gd complex being significantly smaller (Table 2).

Such differences in coordination environments must have an impact on the metal-centred luminescence of the complexes. Due to the unique photophysical properties of REE complexes with heterocycles, the study of the influence of the nature of the ligand and the counter-ion on the photophysical properties of the complexes is of great importance.[53] The difference in the coordination environment is due to the nature of the counter-ion that results in the discrepancy in photophysical properties of the complexes. Moreover, the co-ordinated water molecule suggests quenching of the luminescence of the corresponding complex permanently. The nature of the environment of the europium ion can be obtained through analysis of relative intensities of the transitions of its absorption and luminescence spectra. Absorbance spectra of complexes show very similar information for the complexes with the same type of ligands and are practically independent of the counter-ion (Fig. 5).

The absorbance spectra of complexes **DPPO**Eu(NO$_3$)$_3$ and **DPPO**Eu(TFA)$_3$ have main maxima in the spectral region of 300–310 nm that correspond to absorption by the ligand. For **DPPO**Eu(TFA)$_3$ this maximum shifts 2 nm towards shorter wavelengths. We can see different spectra for complexes **PnPPO**Eu(NO$_3$)$_3$ and **PnPPO**Eu(TFA)$_3$. The absorbance maxima
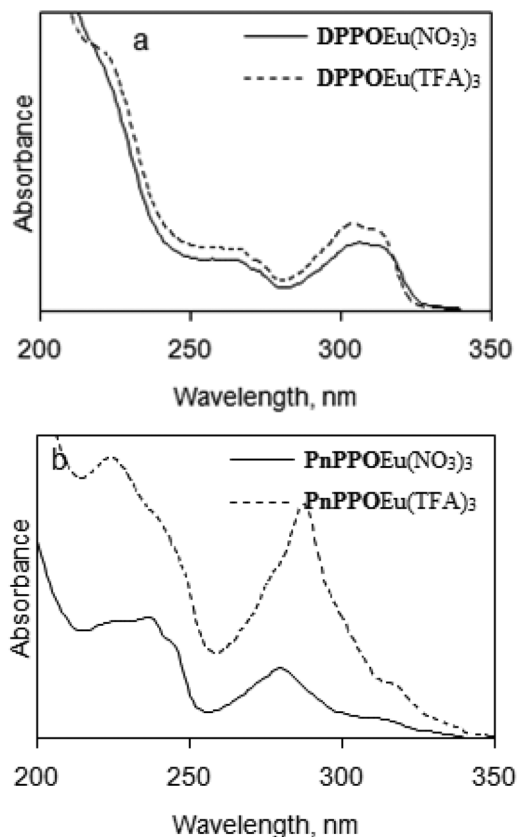
Fig. 5 Absorbance spectra of europium complexes in acetonitrile solutions: (a) **DPPOEu(NO₃)₃**, **DPPOEu(TFA)₃**; (b) **PnPPOEu(NO₃)₃**, **PnPPOEu(TFA)₃**.

the red region that corresponds to transitions $^5D_0 \rightarrow {}^7F_J$ (J = 0–6).[53] In this study we observed only the first five maxima: at wavelength 582 nm ($^5D_0 \rightarrow {}^7F_0$), 595 nm ($^5D_0 \rightarrow {}^7F_1$), 619 nm ($^5D_0 \rightarrow {}^7F_2$), 650 nm ($^5D_0 \rightarrow {}^7F_3$) and in the region 680–710 nm ($^5D_0 \rightarrow {}^7F_4$).

The first transition ($^5D_0 \rightarrow {}^7F_0$) that can be observed at the wavelength 570–585 nm is forbidden by the Judd–Ofelt theory[54] and this transition is an example of a discrepancy with this theory. To determine different Eu(III) species in solution the $^5D_0 \rightarrow {}^7F_0$ transition can also be used. In this work this line was symmetric, and so only one type of europium was present in all the crystals of the complexes studied. The correlation of the wavelength that corresponds to this transition with the ligand coordination number can be suggested.[55]

The second transition ($^5D_0 \rightarrow {}^7F_1$) can be observed at the wavelength 585–600 nm; this is a magnetic dipole transition. Its intensity is perfect for calibration of the luminescence intensity of the europium complex because it is almost constant. Crystal-field splitting of the $^7F_1$ level is directly reflected by the transition and its intensity is the highest if we consider the spectra of solids with a crystal structure and with central symmetry.[56]

The most intensive maxima corresponds to the $^5D_0 \rightarrow {}^7F_2$ transition for all complexes and are called "hypersensitive" due to the fact that the strongest intensity of the maximum depends on the symmetry of the europium ion and the nature of the ligand.[39] This maximum can be found at the wavelength 610–630 nm. The intensity ratio of the transitions $^5D_0 \rightarrow {}^7F_2$ and $^5D_0 \rightarrow {}^7F_1$ is often compared with the intensities of the hypersensitive transition in different europium compounds as an alternative to measure the absolute intensity.[57]

In general the $^5D_0 \rightarrow {}^7F_3$ transition can be observed at the 640–660 nm spectral range and is very weak because it is forbidden. The strong intensity of this transition is a sign of strong crystal-field perturbation.[58]

The $^5D_0 \rightarrow {}^7F_4$ transition corresponds to the luminescence maxima in the spectral range of 680–710 nm.[59] The intensity of the $^5D_0 \rightarrow {}^7F_4$ transition is too low and is very little
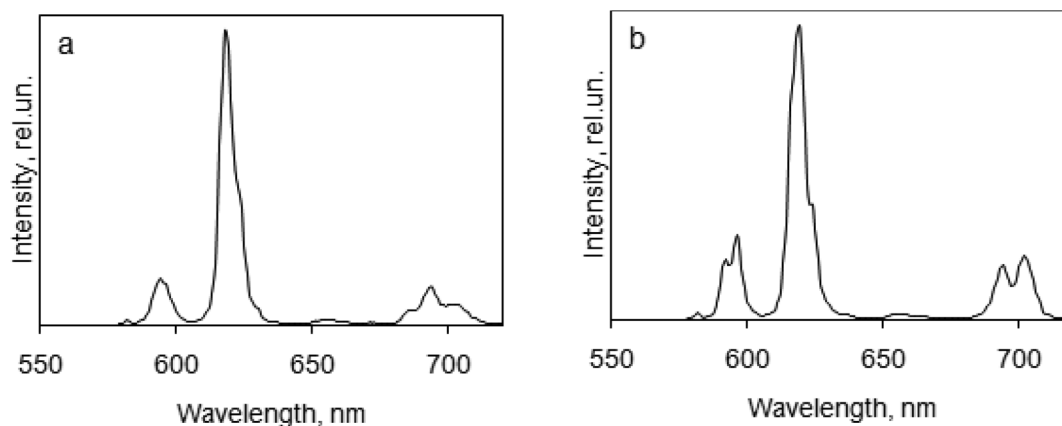
are located in the region of 275–290 nm and the **PnPPOEu(TFA)₃** maximum is shifted 10 nm towards longer wavelengths.

The luminescence spectra for the europium complexes give more information than that obtained from absorption spectra (Fig. 6 and 7). A typical europium emission spectrum shows intense luminescence signals and includes several maxima in

Fig. 6 Luminescence emission spectra of europium complexes in the solid state, λ_{ex} = 270 nm: (a) **DPPOEu(NO₃)₃**; (b) **DPPOEu(TFA)₃**.
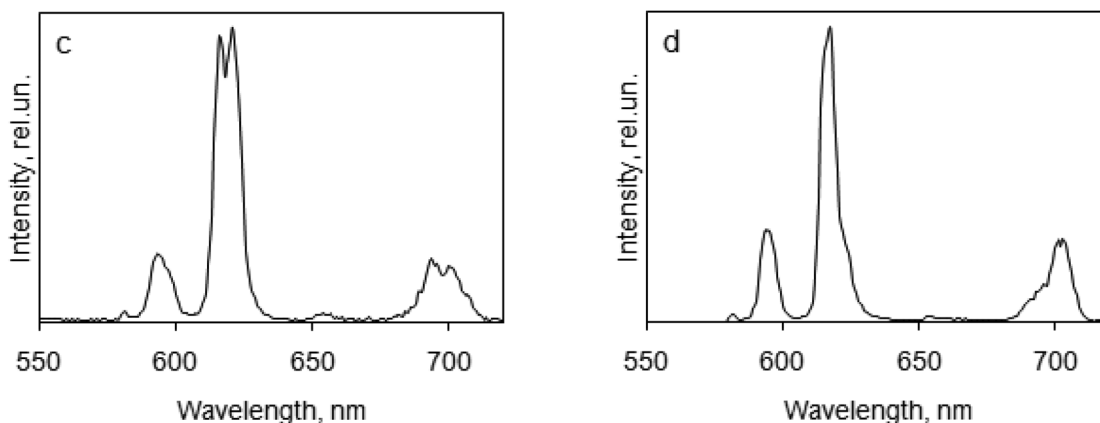
Fig. 7 Luminescence emission spectra of europium complexes in the solid state, λ_{ex} = 270 nm: (c) **PnPPOEu(NO₃)₃**; (d) **PnPPOEu(TFA)₃**.

compared to other transitions, whereas the intensity of this transition is exaggerated in an overcorrected spectrum.

In this study, the $^5D_0 \rightarrow ^7F_5$ transition (740–770 nm) and the $^5D_0 \rightarrow ^7F_6$ transition (810–840 nm) were not observed because the intensities of these transitions are very low.[60] The ratios of intensities corresponding to $^5D_0 \rightarrow ^7F_2$ and $^5D_0 \rightarrow ^7F_1$ transitions are different for the complexes studied: for **DPPOEu(NO₃)₃** and **PnPPOEu(NO₃)₃** they are 6 and 5, respectively, showing deviation from an inversion centre in the complexes.[39] In complexes **DPPOEu(TFA)₃** and **PnPPOEu(TFA)₃** this ratio is ~4, indicating that the deviation is not so strong.

The phosphorescence lifetimes of the $^5D_0$ level in europium complexes in the solid state were 1.20 ± 0.03 ms for **DPPOEu(NO₃)₃**, 2.16 ± 0.06 ms for **DPPOEu(TFA)₃**, 1.01 ± 0.07 ms for **PnPPOEu(NO₃)₃** and 1.84 ± 0.05 ms for **PnPPOEu(TFA)₃**.

Quantum yields of europium complexes were measured using the reference dye method. Rhodamine B was selected as a reference dye because of its high quantum yield value and usability.

The values of luminescence quantum yields for different concentrations were calculated (Fig. 8). For **PnPPOEu(NO₃)₃** the luminescence quantum yield equals to 11% at the concentration 0.1–3.0 × 10⁻⁵ mol L⁻¹ (but concentration depen-

dence was not detected). For other complexes luminescence quenching at concentrations of more than 8.0 × 10⁻⁶ mol L⁻¹ was observed. The maximum luminescence quantum yield was observed for **DPPOEu(NO₃)₃** and **DPPOEu(TFA)₃**: it equalled 85% for both complexes. So the retention of a water molecule in the coordination environment of the europium ion in solution for complex **DPPOEu(TFA)₃** is doubtful, while **PnPPOEu(TFA)₃** seems to keep the water coordinated with the metal ion even in acetonitrile solutions.

The excitation spectra of complexes with the DPPO-type ligand have some maxima that correspond to electronic transitions: $^5L_6 \leftarrow ^7F_0$ (390–405 nm), $^5D_2 \leftarrow ^7F_0$ (460–470 nm), $^5D_1 \leftarrow ^7F_1$ and $^5D_1 \leftarrow ^7F_0$ (520–540 nm) (Fig. 9).

The $^5L_6 \leftarrow ^7F_0$ transition is the most intense in the excitation spectra of europium complexes. Excitation of europium to induce the photoluminescence transitions mentioned above is commonly used if the ligand excitation is forbidden due to the absence of efficient energy transfer. $^5L_6$ level excitation allows direct population of the 4f levels.[61–63] The $^5D_1 \leftarrow ^7F_1$ and $^5D_2 \leftarrow ^7F_0$ transitions are hypersensitive ($J = 2$).
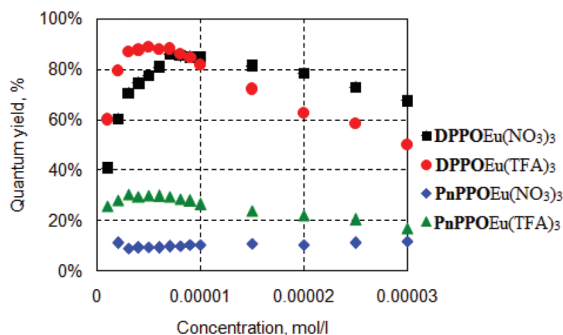

Fig. 8 Dependence of the value of the luminescence quantum yield on the concentration of europium complexes in acetonitrile solutions.
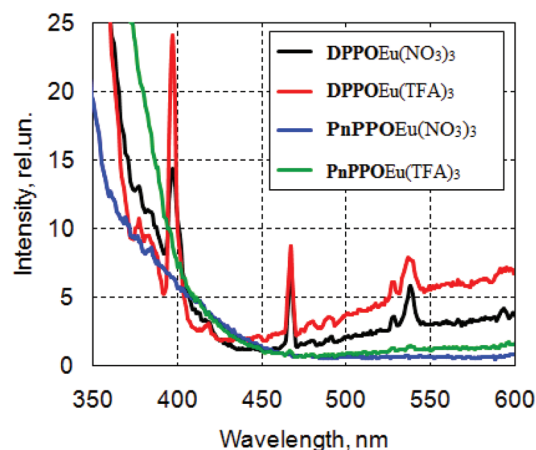

Fig. 9 Luminescence excitation spectra of europium complexes in the solid state at 300 K (λ_{em} = 618 nm).

Conclusions

We successively designed and synthesized two related tetra-dentate N,N',O,O'-ligands based on 2,2′-bipyridyl- and phenanthroline-bearing phosphinoyl-type substituents. The ligands were X-ray characterised and their complexes were studied in respect of the possible difference in metal ion coordination driven by the nature of the counter-ion or geometric rigidity of the ligand. Two examples of complexes with each ligand and every counter-ion (nitrate or trifluoroacetate) were examined by X-ray single-crystal diffraction. The coordination environment of the metal ion is strongly counter-ion dependent. But the conformations of the phosphinoyl groups relative to the pyridine rings depend on the flexibility of the ligand. As a result, the photophysical properties of the complexes are strongly ligand and counter-ion dependent:

• Absorbance and luminescence excitation spectra of complexes showed main peaks in the UV range which correspond to absorption by the ligand and they are ligand-dependent. Luminescence spectra of complexes showed typical europium emissions in the red region, with high quantum yield, that correspond to the transitions $^5D_0 \rightarrow {}^7F_J$ (J = 0–6).

• The value of deviation of the components of $^5D_0 \rightarrow {}^7F_2$ and $^5D_0 \rightarrow {}^7F_1$ transitions from the inversion centre showed a larger dependence on the counter-ion than on the nature of the ligand. Thus the degree of symmetry is more dependent on the counter-ion than on the ligand structure.

• The value of the luminescence quantum yield was the highest for europium complexes with the DPPO ligand and the NO_3 counter-ion; the smallest for complexes with the PhenPPO ligand and the NO_3 counter-ion.

• The value of phosphorescence lifetimes of the $^5D_0$ level in the solid state was higher for complexes with the TFA counter-ion (about 2.0 ms) than for those with the NO_3 counter-ion (about 1.1 ms). A small dependence of the lifetime on the nature of the ligand was demonstrated.

Experimental

General

The NMR spectra were measured with a BRUKER AVANCE-600 (600.12 MHz) NMR spectrometer at 23 °C. Chemical shifts are given in ppm relative to $SiMe_4$ (for ^1H and ^{13}C NMR) and 85% H_3PO_4 (for ^{31}P). IR spectra were recorded with an Agilent 640 FTIR spectrometer with samples in KBr pellets. Mass spectra were obtained with a MALDI-TOF Reflex 3 instrument (BRUKER) in the positive ion mode (UV laser, 337 nm). 6,6′-Dichloro-2,2′-bipyridine,[47] 2,9-dichlorophenanthroline[23] and 2,6-bis(diphenylphosphinoyl)pyridine[50] were prepared according to known procedures. All reagents and solvents were obtained from commercial sources.

For X-ray structure determination the data collection was performed with an APEX II CCD diffractometer. The structure was solved and refined against F^2 by full-matrix least squares techniques with the SHELXTL software package.[64,65]

Crystallographic data, crystal packing, hydrogen bonding information and details of data collection are listed in the ESI.† CCDC 1522002 [for PyPPO], 1522000 [for DPPO], 1521999 [for PnPPO], 1522001 [for 1], 1521997 [for DPPOGd(NO₃)₃] and 1521998 [for PnPPOEu(TFA)₃] contain the supplementary crystallographic data for this paper.

Luminescence properties of complexes were obtained for powdered samples in the solid state and in acetonitrile solution at 300 K using a Hitachi F-7000 luminescence spectrometer. Reflection geometry was used for detecting luminescence spectra of europium complexes in the solid state. Registration of absorbance spectra of europium complex solutions was performed with a Hitachi U-1900 spectrophotometer.

Synthesis of 6,6′-bis(diphenylphosphinoyl)-2,2′-bipyridyl (DPPO). To a stirred mixture of sodium (0.92 g, 0.04 mol) in dry dioxane (30 mL) under argon, a solution of chlorodiphenylphosphine (3.7 mL, 0.02 mol) in dry dioxane (20 mL) was added dropwise over 1 h. After the addition was completed and appearance of a bright yellow coloration was observed, the solution was refluxed for an additional 4 h. Then a solution of 6,6′-dichloro-2,2′-bipyridine (2.25 g, 0.01 mol) in dry dioxane was added dropwise to the solution of sodium diphenylphosphide at 0 °C. The mixture was stirred overnight and treated with three equivalents of hydrogen peroxide to oxidize phosphine groups. Once the reaction was complete, the precipitate of DPPO was filtered off, washed with water and air-dried to afford a white solid (4.4 g, 80%). Found: C, 72.9; H, 4.8; N, 4.98. Calc. for $C_{34}H_{26}N_2O_2P_2$: C, 73.4; H, 4.7; N, 5.0. ν_{max}/cm^{-1} 3076, 3056 ν(C–H), 1569 ν(C=N), 1550, 1436, 1420, 1200 ν(P=O), 1150, 1118, 1099, 1073, 988, 807, 753, 739, 692, 566, 543, and 517. δ_H (CDCl₃) 7.45 (8H, td, J = 7.57, 2.52 Hz, $H_{Ph-3,Ph-5}$), 7.51 (4H, t, J = 6.92 Hz, H_{Ph-4}), 7.91 (8H, dd, J = 11.78, 7.38 Hz, $H_{Ph-2,Ph-6}$), 7.96 (2H, dt, J = 7.75, 3.92 Hz, H_{Py-4}), 8.32 (4H, dd, J = 7.34, 5.70 Hz, $H_{Py-3,Py-5}$). δ_C (CDCl₃) 156.37 (d, $^1J_{CP}$ = 132.0 Hz, C_{Py-6}); 155.36 (d, $^3J_{CP}$ = 18.3 Hz, C_{Py-2}); 137.39 (d, $^2J_{CP}$ = 9.8 Hz, C_{Py-5}); 131.68 (d, $^1J_{CP}$ = 104.5 Hz, C_{Ph-1}); 132.09 (d, $^2J_{CP}$ = 9.2 Hz, C_{Ph-2}); 131.93 (d, $^4J_{CP}$ = 3.0 Hz, C_{Ph-4}); 128.63 (d, $^3J_{CP}$ = 20.0 Hz, C_{Py-4}); 128.32 (d, $^3J_{CP}$ = 12.8 Hz, C_{Ph-3}); 122.58 (d, $^4J_{CP}$ = 3.0 Hz, C_{Py-3}). δ_P (CDCl₃) 21.3. MS (MALDI-TOF) m/z 557 ([M + H⁺], 100%), 579 ([M + Na⁺], 40%). MS (ESI) m/z 557 ([M + H⁺], 100%), 579 ([M + Na⁺], 33%), 595 ([M + K⁺], 40%).

Synthesis of 2,9-bis(diphenylphosphinoyl)phenanthroline (PnPPO). To a stirred mixture of sodium (0.3 g, 13 mmol) in dry dioxane (7 mL) under argon, a solution of chlorodiphenylphosphine (0.74 mL, 4 mmol) in dry dioxane (7 mL) was added. After the addition was complete the mixture was refluxed for an additional 2 h prior to use. Then a solution of 2,9-dichlorophenanthroline (0.5 g, 2 mmol) in 5 ml of dry dioxane was added dropwise to the solution of sodium diphenylphosphide at −18 °C. The mixture was stirred overnight, and then treated with 25 ml of water followed by 150 ml of 5% hydrogen peroxide. Once the reaction was complete (about 30 min), the yellow precipitate of PnPPO was filtered off, washed with water and air-dried (0.8 g, 70%). Found: C, 74.15;

H, 4.5; N, 4.7. Calc. for $C_{36}H_{29}N_2O_2P_2$: C, 74.5; H, 4.5; N, 4.8. δ_H (CDCl$_3$) 8.73 (1H, dd, J = 6.05, 3.90 Hz, H$_{Pn}$), 8.44 (1H, dd, J = 7.93, 3.44 Hz, H$_{Pn}$), 8.08 (4H, dd, J = 10.45, 8.53 Hz, H$_{Ph}$), 7.91 (1H, s, H$_{Pn}$), 7.44 (2H, t, J = 7.20 Hz, H$_{Ph}$), 7.23–7.30 (8H, m, H$_{Ph}$). δ_P (CDCl$_3$) 22.19. δ_C (CDCl$_3$) 157.20 (d, $^1J_{C-P}$ = 131.58 Hz, C$_{Pn2}$), 146.29 (d, $^3J_{C-P}$ = 20.73 Hz, C$_{Pn10b}$), 136.29 (d, $^2J_{C-P}$ = 8.57 Hz, C$_{Pn4a}$), 132.53 (d, $^1J_{C-P}$ = 109.71 Hz, C$_{Ph1}$), 132.13 (d, $^2J_{C-P}$ = 9.12 Hz, C$_{Ph2}$), 131.70 (C$_{Pn5}$), 129.55 (C$_{Ph4}$), 128.38 (d, $^3J_{C-P}$ = 12.16 Hz, C$_{Pn3}$), 128.30 (d, $^3J_{C-P}$ = 13.27 Hz, C$_{Ph3}$), 126.47 (d, $^3J_{C-P}$ = 21.01 Hz, C$_{Pn4}$).

Preparation of the complexes

General synthesis of complexes. To a solution of the ligand (0.1 mmol) in 85 ml dry acetonitrile was added corresponding lanthanide salt hydrate (0.1 mmol) under stirring. The solution was refluxed for 6 hours under stirring. The solution was concentrated in a rotary evaporator while heating. The resulting dry substance was suspended in dry acetonitrile, filtered on a glass filter and washed with acetonitrile. The resulting white powder was air dried, and then kept in a dessicator under paraffin until a constant mass was reached.

DPPOEu(NO$_3$)$_3$ (71 mg, 79%). Found: C, 44.7; H, 3.3; N, 7.2. Calc. for $C_{34}H_{26}EuN_5O_{11}P_2 \cdot H_2O$: C, 44.75; H, 3.1; N, 7.7. ν_{max}/cm^{-1} 3062 ν(C–H), 2931, 2854, 3388 ν(OH), 1143 ν(P=O), 1589 ν(conj. C=N), 746, 728, 692 ν_δ(C–H), 1476 ν(N=O), 1292 ν_a(NO$_2$), 1027 ν_s(NO$_2$). δ_H (acetonitrile-d_3) 5.65 (1H, br.s., H$_{Py}$), 6.26 (6H, br.s., H$_{Ph}$), 6.33 (2H, br.s., H$_{Ph}$), 6.80 (2H, t, J = 7.34 Hz, H$_{Ph}$), 9.04 (1H, br.s., H$_{Py}$), 11.13 (1H, br.s., H$_{Py}$). δ_C (acetonitrile-d_3) 167.01 (br.m., C$_{Py-2}$), 155.92 (br.s., C$_{Py-4}$), 146.12 (d, $^1J_{CP}$ = 119.69 Hz, C$_{Ph-1}$), 133.53 (s. C$_{Ph-4}$), 129.12 (d, $^2J_{CP}$ = 9.67 Hz, C$_{Ph-2}$), 128.26 (d, $^3J_{CP}$ = 12.16 Hz, C$_{Ph-3}$), 112.01 (d, $^1J_{CP}$ = 108.08 Hz, C$_{Py-6}$), 110.78 (s, C$_{Py-3}$), 100.91 (d, $^3J_{CP}$ = 16.59 Hz, C$_{Py-5}$). δ_P (acetonitrile-d_3) 60.22. MS (MALDI-TOF) m/z 832 ([**DPPOEu(NO$_3$)$_2$**$^+$], 100%).

DPPOGd(NO$_3$)$_3$ (71 mg, 79%). Found: C, 45.7; H, 3.2; N, 7.4. Calc. for $C_{34}H_{26}GdN_5O_{11}P_2$: C, 45.4; H, 2.9; N, 7.8. MS (MALDI-TOF) m/z 838 ([**DPPOGd(NO$_3$)$_2$**$^+$], 100%).

DPPOEu(TFA$_3$) (80 mg, 76%). Found: C, 45.8; H, 2.5; N, 2.6. Calc. for $C_{40}H_{26}EuF_9N_2O_8P_2$: C, 45.9; H, 2.5; N, 2.7. ν_{max}/cm^{-1} 3061, 2927, 2855 ν(C–H), 1200 ν(CF$_3$), 1144vs ν(P=O), 1589vs ν(C=N), 748, 729, 721, 692 ν_δ(C–H), 1440s ν_s(COO), 1707s ν_a(COO). δ_H (acetonitrile-d_3) 9.36 (1H, br.s., H$_{Py-3}$), 8.56 (1H, br. s., H$_{Py-4}$), 7.24 (3H, br.m., H$_{Py-5}$, H$_{Ph-4}$), 6.78 (4H, br.s., H$_{Ph-3}$), 5.62 (4H, br.s., H$_{Ph-2}$). δ_C (acetonitrile-d_3) 169.98 (br.m., C$_{Py-2}$), 153.97 (d, $^3J_{CP}$ = 9.18 Hz, C$_{Py-4}$), 149.64 (d, $^1J_{CP}$ = 126.2 Hz, C$_{Ph-1}$), 134.32 (s, C$_{Ph-4}$), 131.84 (d, $^2J_{CP}$ = 10.32 Hz, C$_{Ph-2}$), 129.34 (d, $^3J_{CP}$ = 12.62 Hz, C$_{Ph-3}$), 116.46 (d, $^1J_{CP}$ = 108.99 Hz, C$_{Py-2}$), 108.32 (s, C$_{Py-3}$), 101.90 (d, $^2J_{CP}$ = 21.80 Hz, $_{CPy-5}$). MS (MALDI-TOF) m/z 935 ([**DPPOEu(TFA)$_2$**$^+$], 15%), 822 ([**DPPOEu(TFA)**$^+$], 20%), 747 ([**DPPOEuF$_2$**$^+$], 20%), 728 ([**DPPOEuF**$^+$], 100%).

PnPPOEu(NO$_3$)$_3$ (72 mg, 78%). Calc. for $C_{36}H_{26}EuN_5O_{11}P_2$: C, 47.1; H, 2.85; N, 7.6. ν_{max}/cm^{-1} 3058, 2927, 2852 ν(C–H), 1564, 1554, 1540 ν(conj. C=N, C-CAr), 1172s ν(P=O), 1439vs ν(N=O), 1194s ν_a(NO$_2$), 1097s ν_s(NO$_2$). δ_H (acetonitrile-d_3) 8.63 (1H, br.s.), 8.08 (4H, br.s.),

7.54 (3H, br.s.), 7.35 (5H, br.s.). δ_P (acetonitrile-d_3) 48. MS (MALDI-TOF) m/z 857 ([**PnPPOEu(NO$_3$)$_2$**$^+$], 30%), 795 ([**PnPPOEu(NO$_3$)**$^+$], 100%).

PnPPOLa(NO$_3$)$_3$ (77 mg, 85%). Found C, 47.5; H, 3.0; N, 7.9. Calc. for $C_{36}H_{26}LaN_5O_{11}P_2$: C, 47.75; H, 2.9; N, 7.7. δ_P (acetonitrile-d_3) 41. MS (MALDI-TOF) m/z 843 ([**PnPPOLa(NO$_3$)$_2$**$^+$], 100%).

PnPPOEr(NO$_3$)$_3$ (75 mg, 80%). Found C, 46.5; H, 2.6; N, 7.3. Calc. for $C_{36}H_{26}ErN_5O_{11}P_2$: C, 46.3; H, 2.8; N, 7.5. MS (MALDI-TOF) m/z 872 ([**PnPPOEr(NO$_3$)$_2$**$^+$], 100%).

PnPPOEu(TFA$_3$)·H$_2$O (74 mg, 69%) Found C, 46.8; H, 2.9; N, 2.9. Calc. for $C_{42}H_{26}EuF_9N_2O_8P_2$: C, 47.1; H, 2.45; N, 2.6. ν_{max}/cm^{-1} 3066, 2929, 2856 ν(C–H), 1677vs ν_a(COO), 1438s ν_s(COO), 1206s ν(CF$_3$), 1141vs ν(P=O). δ_H (acetonitrile-d_3) 8.98 (1H, br.s., H$_{Pn-3}$), 8.76 (1H, br.s., H$_{Pn-5}$), 7.70 (1H, br.s., H$_{Pn-4}$), 7.37 (2H, t, J = 7.34 Hz, H$_{Ph-4}$), 6.94 (4H, br.s., H$_{Ph-3}$), 6.29 (4H, br.s., H$_{Ph-2}$). δ_C (acetonitrile-d_3) 170.09 (br.s., C$_{Pn-10b}$), 152.56 (d, $^3J_{CP}$ = 4.59 Hz, C$_{Pn-2}$), 146.10 (d, $^1J_{CP}$ = 113.58 Hz, C$_{Ph-1}$), 133.53 (s, C$_{Ph-4}$), 131.48 (d, $^2J_{CP}$ = 11.47 Hz, C$_{Ph-2}$), 128.52 (d, $^3J_{CP}$ = 12.62 Hz, C$_{Ph-3}$), 116.27 (d, $^1J_{CP}$ = 108.99 Hz, C$_{Pn-2}$), 114.19 (s, C$_{Pn-4a}$), 93.86 (d, $^2J_{CP}$ = 17.21 Hz, $_{CPn-3}$).

Notes and references

1 J.-C. G. Bunzli and C. Piguet, *Chem. Soc. Rev.*, 2005, **34**, 1048–1077.

2 J.-C. G. Bunzli, *Spectroscopic Properties of Rare Earths in Optical Materials*, ed. G. K. Liu and B. Jacquier, Springer Verlag, Berlin, 2005, ch. 11, vol. 83.

3 J.-C. G. Bünzli, *Chem. Rev.*, 2010, **110**, 2729–2755.

4 J. C. G. Bünzli, in *Spectroscopic Properties of Rare Earths in Optical Materials*, ed. R. Hull, J. Parisi, R. M. Osgood Jr., H. Warlimont, G. Liu and B. Jacquier, Springer, Berlin Heidelberg, 2005, ch. 9, vol. 83, pp. 462–499.

5 J.-C. G. Bunzli, L. J. Charbonniere and R. F. Ziessel, *J. Chem. Soc., Dalton Trans.*, 2000, 1917–1923.

6 J.-C. G. Bünzli, S. Comby, A.-S. Chauvin and C. D. B. Vandevyver, *J. Rare Earths*, 2007, **25**, 257–274.

7 A. Bhattacharyya, P. K. Mohapatra and V. K. Manchanda, *Radiochim. Acta*, 2010, **98**, 141–147.

8 M. G. B. Drew, M. R. S. J. Foreman, C. Hill, M. J. Hudson and C. Madic, *Inorg. Chem. Commun.*, 2005, **8**, 239–241.

9 M. Alyapyshev, V. Babain, N. Borisova, I. Eliseev, D. Kirsanov, A. Kostin, A. Legin, M. Reshetova and Z. Smirnova, *Polyhedron*, 2010, **29**, 1998–2005.

10 P. D. Beer, M. R. Sambrook and D. Curiel, *Chem. Commun.*, 2006, 2105–2117.

11 S. Huh, S. Jung, Y. Kim, S.-J. Kim and S. Park, *Dalton Trans.*, 2010, **39**, 1261–1265.

12 Z. Kolarik, *Chem. Rev.*, 2008, **108**, 4208–4252.

13 L. N. Puntus, K. A. Lyssenko, M. Y. Antipin and J.-C. G. Bünzli, *Inorg. Chem.*, 2008, **47**, 11095–11107.

14 S. Mishra, G. Ledoux, E. Jeanneau, S. Daniele and M.-F. Joubert, *Dalton Trans.*, 2012, **41**, 1490–1502.

15 Y. P. Du, Y. W. Zhang, L. D. Sun and C. H. Yan, *J. Phys. Chem. C*, 2008, **112**, 405–415.

16 J. C. Boyer, F. Vetrone, L. A. Cuccia and J. A. Capobianco, *J. Am. Chem. Soc.*, 2006, **128**, 7444–7445.

17 J. C. Boyer, L. A. Cuccia and J. A. Capobianco, *Nano Lett.*, 2007, **7**, 847–852.

18 F. de Maria Ramírez, L. Charbonnière, G. Muller, R. Scopelliti and J.-C. G. Bünzli, *J. Chem. Soc., Dalton Trans.*, 2001, 3205–3213.

19 F. Renaud, C. Piguet, G. Bernardinelli, G. Hopfgartner and J.-C. G. Bunzli, *Chem. Commun.*, 1999, 457–458.

20 S. Petoud, J.-C. G. Bünzli, T. Glanzman, C. Piguet, Q. Xiang and R. P. Thummel, *J. Lumin.*, 1999, **82**, 69–79.

21 F. Avecilla, C. Platas-Iglesias, R. Rodríguez-Cortiñas, G. Guillemot, J.-C. G. Bünzli, C. D. Brondino, C. F. G. C. Geraldes, A. de Blas and T. Rodríguez-Blas, *J. Chem. Soc., Dalton Trans.*, 2002, 4658–4665.

22 A.-S. Chauvin, J.-C. G. Bünzli, F. Bochud, R. Scopelliti and P. Froidevaux, *Eur. J. Chem.*, 2006, **12**, 6852–6864.

23 M. Galletta, S. Scaravaggi, E. Macerata, A. Famulari, A. Mele, W. Panzeri, F. Sansone, A. Casnati and M. Mariani, *Dalton Trans.*, 2013, **42**, 16930–16938.

24 T. Kobayashi, T. Yaita, S. Suzuki, H. Shiwaku, Y. Okamoto, K. Akutsu, Y. Nakano and Y. Fujii, *Sep. Sci. Technol.*, 2010, **45**, 2431–2436.

25 D. Manna, S. Mula, A. Bhattacharyya, S. Chattopadhyay and T. K. Ghanty, *Dalton Trans.*, 2015, **44**, 1332–1340.

26 D. Merrill and R. D. Hancock, *Radiochim. Acta*, 2011, **99**, 161–166.

27 C.-L. Xiao, C.-Z. Wang, L.-Y. Yuan, B. Li, H. He, S. Wang, Y.-L. Zhao, Z.-F. Chai and W.-Q. Shi, *Inorg. Chem.*, 2014, **53**, 1712–1720.

28 X. Zhang, L. Yuan, Z. Chai and W. Shi, *Sep. Purif. Technol.*, 2016, **168**, 232–237.

29 C.-L. Xiao, C.-Z. Wang, L. Mei, X.-R. Zhang, N. Wall, Y.-L. Zhao, Z.-F. Chai and W.-Q. Shi, *Dalton Trans.*, 2015, **44**, 14376–14387.

30 J. L. Lapka, A. Paulenova, R. S. Herbst and J. D. Law, *Sep. Sci. Technol.*, 2010, **45**, 1706–1710.

31 C. Marie, M. Miguirditchian, D. Guillaneux, J. Bisson, M. Pipelier and D. Dubreuil, *Solvent Extr. Ion Exch.*, 2011, **29**, 292–315.

32 C. Marie, M. Miguirditchian, D. Guillaumont, A. Tosseng, C. Berthon, P. Guilbaud, M. Duvail, J. Bisson, D. Guillaneux, M. Pipelier and D. Dubreuil, *Inorg. Chem.*, 2011, **50**, 6557–6566.

33 N. Boubals, M. G. B. Drew, C. Hill, M. J. Hudson, P. B. Iveson, C. Madic, M. L. Russell and T. G. A. Youngs, *J. Chem. Soc., Dalton Trans.*, 2002, 55–62.

34 N. E. Borisova and M. D. Reshetova, *Russ. Chem. Bull.*, 2015, **64**, 1882–1890.

35 M. Y. Alyapyshev, V. A. Babain, L. I. Tkachenko, A. Paulenova, A. A. Popova and N. E. Borisova, *Solvent Extr. Ion Exch.*, 2014, **32**, 138–152.

36 D. O. Kirsanov, N. E. Borisova, M. D. Reshetova, A. V. Ivanov, L. A. Korotkov, I. I. Eliseev, M. Y. Alyapyshev, I. G. Spiridonov, A. V. Legin, Y. G. Vlasov and V. A. Babain, *Russ. Chem. Bull.*, 2012, **61**, 881–890.

37 M. Y. Alyapyshev, V. A. Babain, N. E. Borisova, R. N. Kiseleva, D. V. Safronov and M. D. Reshetova, *Mendeleev Commun.*, 2008, **18**, 336–337.

38 *Reprocessing and recycling of spent nuclear fuel*, ed. R. Taylor, Woodhead Publishing, 80 High Street, Sawston, Cambridge, CB22 3HJ, UK, 2015.

39 N. E. Borisova, A. A. Kostin, E. A. Eroshkina, M. D. Reshetova, K. A. Lyssenko, E. N. Spodine and L. N. Puntus, *Eur. J. Inorg. Chem.*, 2014, 2219–2229.

40 L. Prodi, M. Montalti, N. Zaccheroni, G. Pickaert, L. Charbonniere and R. Ziessel, *New J. Chem.*, 2003, **27**, 134–139.

41 M. Pietraszkiewicz, A. Kłonkowski, K. Staniszewski, J. Karpiuk and S. Bianketti, *J. Alloys Compd.*, 2004, **380**, 241–247.

42 O. Pietraszkiewicz, M. Pietraszkiewicz, J. Karpiuk and M. Jesie, *J. Rare Earths*, 2009, **27**, 584–587.

43 M. A. Goni, L. M. Daniels and T. A. Siddiquee, *Inorg. Chim. Acta*, 2013, **394**, 645–648.

44 Z. Spichal, M. Necas, J. Pinkas and J. Novosad, *Inorg. Chem.*, 2004, **43**, 2776–2778.

45 M. Correa-Ascencio, E. K. Galván-Miranda, F. Rascón-Cruz, O. Jiménez-Sandoval, S. J. Jiménez-Sandoval, R. Cea-Olivares, V. Jancik, R. A. Toscano and V. García-Montalvo, *Inorg. Chem.*, 2010, **49**, 4109–4116.

46 L. J. Charbonniere, S. Mameri, D. Flot, F. Waltz, C. Zandanel and R. F. Ziessel, *Dalton Trans.*, 2007, 2245–2253.

47 W.-J. Wang, Y.-C. Wang and H.-C. Kao, *J. Chin. Chem. Soc.*, 2010, **57**, 876–882.

48 H. C. Guo, R. H. Zheng and H. J. Jiang, *Org. Prep. Proced. Int.*, 2012, **44**, 392–396.

49 M. Yamada, Y. Nakamura, S. Kuroda and I. Shimao, *Bull. Chem. Soc. Jpn.*, 1990, **63**, 2710–2712.

50 G. R. Newkome and D. C. Hager, *J. Org. Chem.*, 1978, **43**, 947–949.

51 H. K. Wang, *Acta Chem. Scand.*, 1965, **19**, 879.

52 A. L. Rheingold, L. M. Liable-Sands and S. Trofimenko, *Angew. Chem., Int. Ed.*, 2000, **39**, 3321–3324.

53 K. Binnemans, *Coord. Chem. Rev.*, 2015, **295**, 1–45.

54 B. M. Walsh, *Judd-Ofelt theory: principles and practices*, Springer, 2006.

55 G. R. Choppin and Z. M. Wang, *Inorg. Chem.*, 1997, **36**, 249–252.

56 M. M. Murali, M. L. Rama, D. Ramachari and C. K. Jayasankar, *Spectrochim. Acta, Part A*, 2014, **118**, 966–971.

57 G. P. Pires, I. F. Costa, H. F. Brito, W. N. Faustino and E. E. S. Teotonio, *Dalton Trans.*, 2016, **45**, 10960–10968.

58 X. Y. Chen and G. K. Liu, *J. Solid State Chem.*, 2005, **178**, 419–428.

59 M. Xie, Y. Li and R. Li, *J. Lumin.*, 2013, **136**, 303–306.

60 V. I. Verlan, M. S. Iovu, I. Culeac, O. Bordian, V. E. Zubareva and I. Nistor, *IFMBE Proc.*, 2016, **55**, 17–20.

61 V. Tsaryuk, V. Zolin and J. Legendziewicz, *J. Lumin.*, 2003, **102–103**, 744–750.

62 O. L. Malta and F. R. Gonçalves e Silva, *Spectrochim. Acta, Part A*, 1998, **54**, 1593–1599.

63 C. A. Kodaira, H. F. Brito, O. L. Malta and O. A. Serra, *J. Lumin.*, 2003, **101**, 11–21.

64 G. M. Sheldrick, *SHELXS97. Program for the Solution of Crystal Structures*, University of Göttingen, Göttingen, Germany, 1997.

65 G. M. Sheldrick, *SHELXL97. Program for the Refinement of Crystal Structures*, University of Göttingen, Göttingen, Germany, 1997.